CRYSTAL GROWTH & DESIGN
2008
VOL. 8, NO. 9
3408–3414

Potential of Chiral Solvents for Enantioselective Crystallization. 1. Evaluation of Thermodynamic Effects

Samuel Kofi Tulashie,*[,†] Heike Lorenz,[†] Liane Hilfert,[‡] Frank Thomas Edelmann,[‡] and Andreas Seidel-Morgenstern[†,‡]

Max Planck Institute for Dynamics of Complex Technical Systems, Magdeburg, Germany, and Otto-von-Guericke-Universität Magdeburg, Magdeburg, Germany

Received April 7, 2008; Revised Manuscript Received May 28, 2008

ABSTRACT: It can be expected that a chiral solvent possesses a certain potential to discriminate between two enantiomers by creating specific weak interactions and forming diastereomeric complexes which have different physical properties. Thus, for chiral solvents, there might be an asymmetry in the solubility phase diagrams that could be employed for resolution purposes. In this work, investigations were carried out to identify appropriate chiral solvents for the discrimination of enantiomers with the aid of nuclear magnetic resonance (NMR) spectroscopy and Raman spectroscopy. The ^{1}H NMR and Raman spectra results of mandelic acid in the chiral solvents did not show any significant chiral recognition. The effect of (*S*)-ethyl lactate and (2*R*, 3*R*)-diethyl tartrate on solubility was examined by measuring the ternary phase diagrams of mandelic acid and *N*-methylephedrine. The phase diagrams determined at different temperatures were symmetric indicating again that the used chiral solvents have less or no influence on the thermodynamics of solution. However, in additional experiments, it was found that there can be significant differences in the nucleation behavior of the two enantiomers in a chiral solvent.

Introduction

The importance of enantioseparation increases because of the fact that the introduction of racemic drugs is more and more restricted by the regulatory agencies. As a result, the manufacture of pure enantiomer drugs is of large interest for the pharmaceutical industry.[1,2] Normally, a racemate, i.e., a 50:50 mixture of both enantiomers is produced after a chemical synthesis of optically active molecules. Typically, only one of the enantiomers exhibits the desired physiological effect. This has necessitated the resolution of racemic mixtures and compounds into single enantiomers. Since 1990, the section of drugs marketed as pure enantiomer drugs exceeds the section of racemic mixtures.[2,3] On the basis of these reasons, the importance and application ranges of enantioseparation have increased steadily in the pharmaceutical industry.

In principle, diastereomeric interactions can be formed when enantiomers are dissolved in an optically active solvent.[4] These diastereomeric complexes should possess different physical and chemical properties.

Because a chiral solvent has the potential to discriminate between two enantiomers, asymmetry could be induced in a solubility phase diagram. Based on this asymmetry, the resolution of a racemic mixture should be feasible by direct crystallization. It is usually assumed that the possibility to resolve a racemic mixture by direct crystallization is given only when it crystallizes as a conglomerate. An elegant separation process used to separate racemic mixtures of enantiomers is preferential crystallization,[5] which is up to now only applicable to conglomerate systems. Unfortunately, only approximately 5% of the known enantiomeric systems exhibit this behavior.[6] On this basis, more effort is focused to develop resolution processes capable to resolve compound forming systems, e.g., continuous enantioseparation with enantioselective membranes,[7] preferential crystallization in racemic compound forming systems,[8,9] and supramolecular complexation with chiral host molecules.[10] We started in our laboratory to investigate the ability of chiral solvents to discriminate between enantiomers through crystallization procedures. Despite the fact that this concept has been considered as a relevant tool since the beginning of the 20th century, only a few studies can be found in the literature.[11–17] For example, Yamamoto et al. reported solubility differences in the case of a chiral cobalt salt in pure enantiomeric diethyl tartrate.[16] Amaya evaluated theoretically this solubility difference between two pure enantiomers in a chiral solvent.[17] To evaluate the potential of this promising concept further, more systematic experimental work is required, which is the focus of this work.

To systematically study the feasibility of chiral resolution with the help of chiral solvents, we first screened a variety of chiral solvents that would be suitable for chiral discrimination. Further experiments to investigate interactions between mandelic acid and the chosen chiral solvents were carried out with Raman spectroscopy. Mandelic acid, a compound forming system, was chosen as a typical chiral system for the screening and the interaction measurements. Ternary solubility phase diagrams were determined for mandelic acid (MA) and the conglomerate forming system *N*-methylephedrine (NME) in (*S*)-ethyl lactate (EL) and (2*R*, 3*R*)-diethyl tartrate (DT) as selected chiral solvents. Finally, a few nucleation tests were done in order to assess the possibility of a kinetically driven resolution.

Experimental Section

Chemicals. Mandelic acid (enantiopure and racemic), *N*-methylephedrine (enantiopure), (*S*)-(−)-ethyl lactate, and (2*R*, 3*R*)-(+)-diethyl tartrate obtained from Aldrich or Merck with purities ≥99% were used. For the ^{1}H NMR experiments, Methanol-d_4 obtained from Deutero GmbH with purity ≥99.8% was used. A variety of seven chiral solvents was also applied for the screening experiments: (*S*)-2-butanol, (*S*)-2-pentanol, (*S*)-2-hexanol, (*S*)-1-phenylethanol, (*R*)-1-phenylethanol, (*R*)-2-chloro-1-(3-chlorophenyl)ethanol, and (*R*)-2-chloro-1-phenylethanol. All were provided from BASF AG and of purity ≥99%.

* Corresponding author Address: Max Planck Institute for Dynamics of Complex Technical Systems, Sandtorstrasse 1, D-39106 Magdeburg, Germany. Phone: (0049) 391 6110 287. Fax: (0049) 391 6110 524. E-mail: tulashie@mpi-magdeburg.mpg.de.
† Max Planck Institute for Dynamics of Complex Technical Systems.
‡ Otto-von-Guericke-Universität Magdeburg.

10.1021/cg800356v CCC: $40.75
Published on Web 07/23/2008

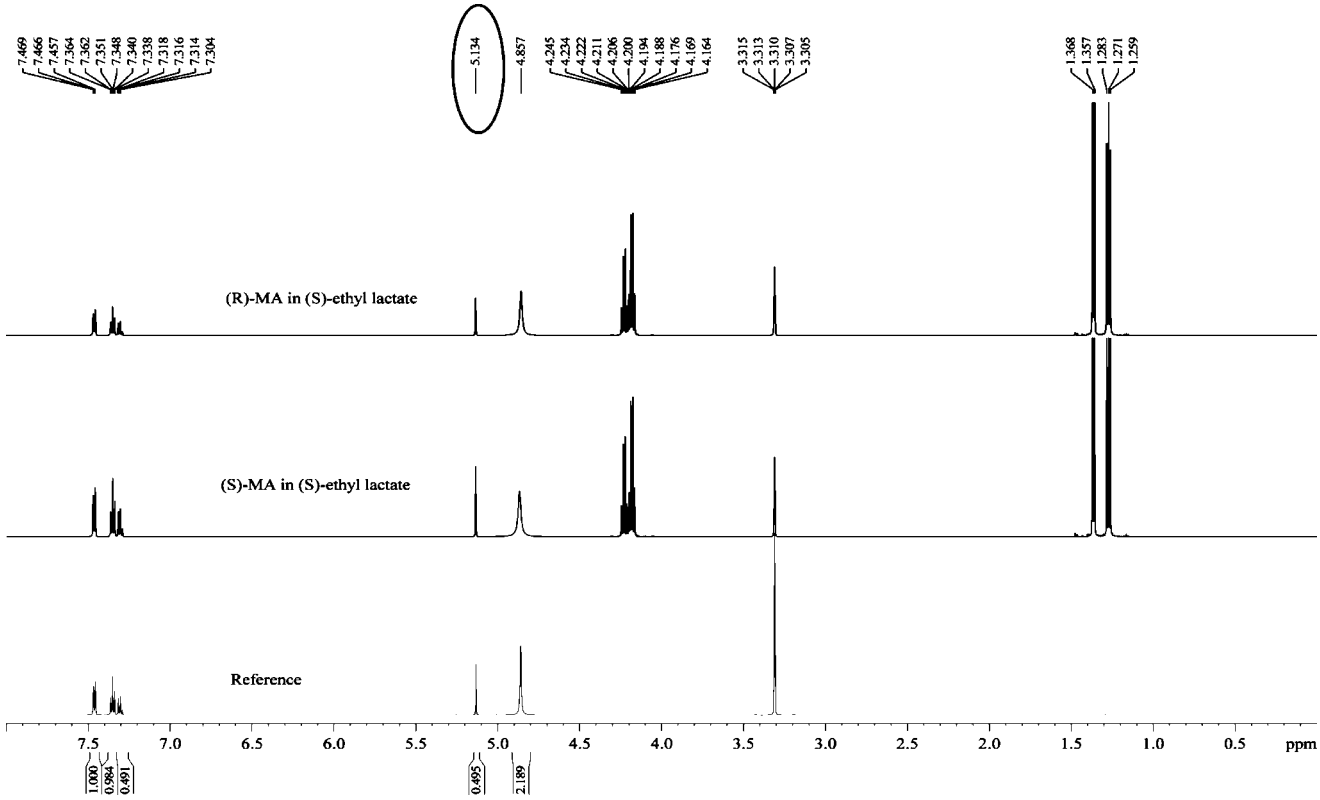

Figure 1. [1]H NMR spectra for mandelic acid in (*S*)-ethyl lactate.

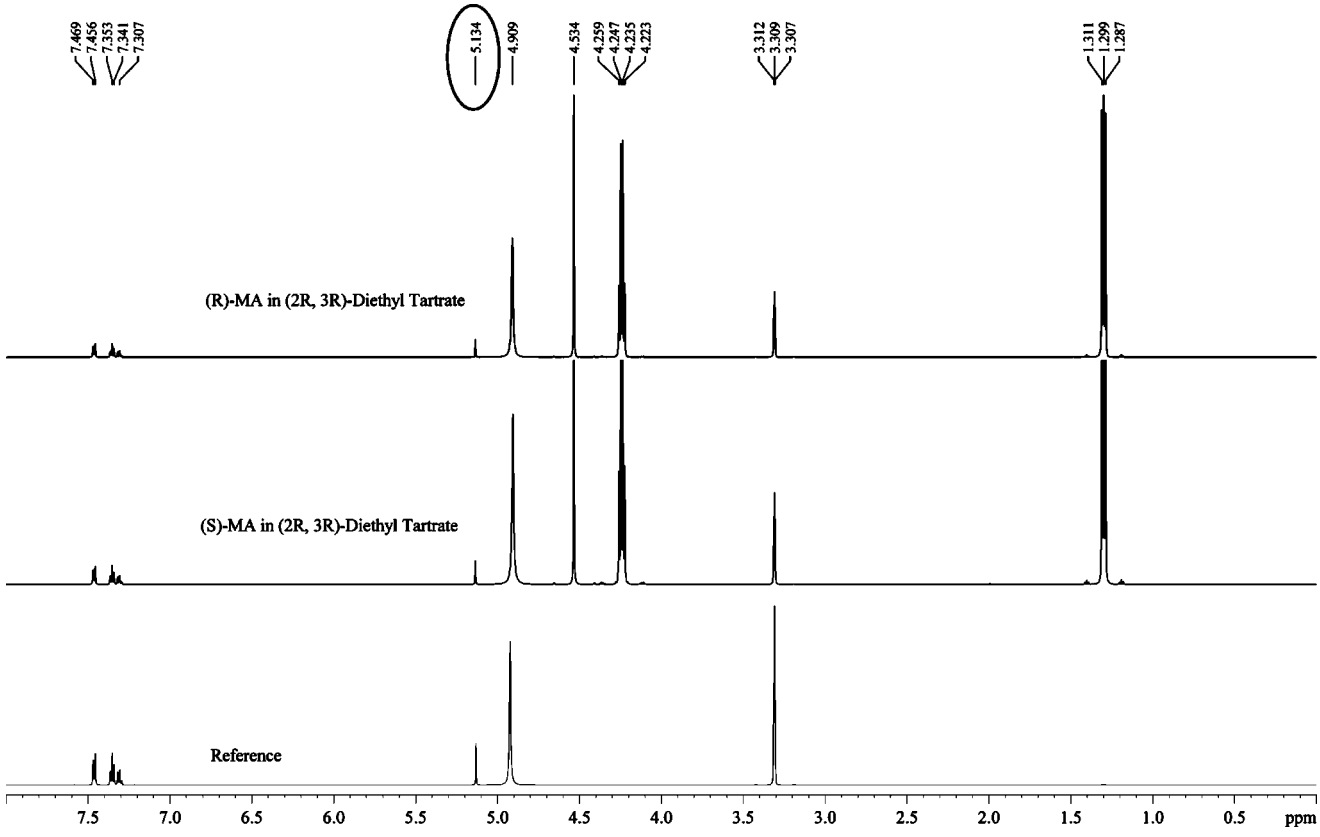

Figure 2. [1]H NMR spectra for mandelic acid in (2*R*, 3*R*)-diethyl tartrate.

Analytical Methods. Because there are no systematic experimental works on this subject, the available analytical techniques used in the present work will be discussed in some detail in this section.

[1]H NMR Measurements. [1]H NMR spectra were recorded on a Bruker AVANCE 600 spectrometer at 600.13 MHz. The AVANCE 600 is fitted with a 5 mm CPTXI-1H-13C/15N/2H probe head with

Table 1. Screened Chiral Solvents and the Resulting Chemical Shifts

chiral solvents	(*S*)-MA[a] alpha hydrogen peak (ppm)	(*R*)-MA alpha hydrogen peak (ppm)	(*S*)-MA $\Delta\delta$ values (ppm)	(*R*)-MA $\Delta\delta$ values (ppm)	reference sample α hydrogen peak (ppm)
(*S*)-ethyl lactate	5.13	5.13	0.00	0.00	5.13
(*S*)-2-butanol	5.05	5.05	0.00	0.00	5.05
(*S*)-2-pentanol	5.07	5.06	0.00	0.01	5.07
(*S*)-2-hexanol	5.13	5.13	0.00	0.00	5.13
(*S*)-1-phenylethanol	5.14	5.14	0.01	0.01	5.13
(*R*)-1-phenylethanol	5.14	5.14	0.01	0.01	5.13
(*R*)-2-chloro-1-(3-chlorophenyl)ethanol	5.14	5.14	0.01	0.01	5.13
(2*R*, 3*R*)-diethyl tartrate	5.13	5.13	0.00	0.00	5.13
(*R*)-2-chloro-1-phenylethanol	5.14	5.14	0.01	0.01	5.13

[a] MA = Mandelic acid.

z-gradients. The sample was measured in methanol-d_4 deuterated solvent as internal lock. Spectra were recorded at $T = 293$K with a pulse width of 7.8 μs for 90° pulse. The ^{1}H NMR chemical shifts (δ) were reported in parts per million downfield from TMS (internal).[18,19]

The following samples were prepared in NMR tubes:

Test samples: (a) (*S*)-mandelic acid (10 mM) + (*S*)-ethyl lactate (50 mM) + CD_3OD (600 μL)

(b) (*R*)-mandelic acid (10 mM) + (*S*)-ethyl lactate (50 mM) + CD_3OD (600 μL)

Reference sample: (*R*)-mandelic acid (10 mM) + CD_3OD (600 μL). The same procedure is repeated for the other chiral solvents studied.

Raman Measurements. Raman spectra were collected with a RAMAN RXN 1 spectrometer from Kaiser Optical Systems Inc. The system employed a laser beam at 785 nm operating at 300 mW. The analyses were carried out for liquid phase samples at ambient temperature. The samples were scanned for a period of 10 s, the resolution was at 4 cm^{-1}. Liquid phase samples of (*S*)- and (*R*)-mandelic acid in both (*S*)-ethyl lactate and (2*R*, 3*R*)-diethyl tartrate at a concentration of 8 wt % were used.

Solubility Equilibria Measurements. An isothermal measurement technique was used to determine the solubilities. It involves preparing a solvent−solute mixture of known composition. These mixtures were placed into a glass vessel with a magnetic stirrer. A preliminary homogeneous state was reached by gently heating and stirring, followed by cooling down under stirring to the set temperature. Afterward, liquid samples were isolated by filtration through a glass filter (pore size 10 μm). Equilibrated crystallized materials were analyzed with HPLC and XRPD. The experiments lasted for 24 h to ensure equilibration. Measurements were repeated at least two times.

Liquid Phase Analysis. The liquid samples collected from the solubility experiments were diluted with isopropanol. The concentration of the solution and the enantiomeric excess were determined with HPLC:

An Agilent HP 1100 unit with a Chiralcel OD-H column (Astec, 250 × 4.6 mm/5 μm) for mandelic acid analyses and a Eurocel OD column (Knauer, 250 × 4.6 mm/5 μm) for *N*-methylephedrine analyses was used. The column temperature was 25 °C and the flow rate 1.0 mL/min. A UV diode array detector was used for peak detection at a wavelength of 254 nm. The eluent compositions were as follows:

(a) Mandelic acid in (*S*)-ethyl lactate: 84% *n*-hexane, 16% isopropanol, and 0.1% trifluoroacetic acid.

(b) Mandelic acid in (2*R*, 3*R*)-diethyl tartrate: 90% *n*-hexane, 10% isopropanol, and 0.1% trifluoroacetic acid.

(c) *N*-Methylephedrine in (*S*)-ethyl lactate and (2*R*, 3*R*)-diethyl tartrate: 85% *n*-hexane, 15% isopropanol, and 0.1% diethylamine.

Solid Phase Analysis. A possible formation of solvates and/or polymorphs in the chiral systems studied was verified analyzing the solid phases by X-ray powder diffraction (XRPD). Crystalline materials were characterized on a PANalytical X'Pert Pro diffractometer (PANalytical GmbH) with Cu Kα radiation and compared with reference patterns. The samples were measured on Si sample holders and scanned from a diffraction angle of 3 to 40° with step size of 0.017° and counting time of 50s per step.

Nucleation Experiments. Primary nucleation experiments were performed for racemic-MA, (*S*)-MA and (*R*)-MA in (*S*)-ethyl lactate using an isothermal method. The experiments were conducted in a magnetically stirred double jacketed glass vessel of 50 mL. Saturated solutions of about 10 g (15 °C) were prepared for all the samples. The various saturated solutions were crash-cooled to −5.0 °C, and the induction time (t_{ind}) at this temperature for the appearance of first crystals was determined by visual observation.

Results and Discussion

The following section comprises results for the screened chiral solvents and the Raman spectra of (*S*)- and (*R*)-MA in both (*S*)-ethyl lactate and (2*R*, 3*R*)-diethyl tartrate to evaluate the presence or absence of chiral interactions. Afterward, the measured ternary solubility phase diagrams are illustrated showing solubility isotherms at different temperatures together with the results of the solid phase analyses by XRPD.

Screening of the Chiral Solvents by Using ^{1}H NMR Spectroscopy. For screening nine chiral solvents were used. The screening experiments were carried out to be able to select the appropriate chiral solvent, which has the potential to create chiral recognition.[20,21]

Figures 1 and 2 exemplarily show the ^{1}H NMR spectra for mandelic acid in (*S*)-ethyl lactate and (2*R*, 3*R*)-diethyl tartrate respectively. It can be seen that in both Figures 1 and 2 there are no differences in the chemical shift between the alpha hydrogen (5.134 ppm) of the reference and that of the test samples.

The screening experiment was based on discrimination definition of the alpha hydrogen of the reference sample (5.134 ppm) and that of the test sample in the chiral solvent, and which is expressed as the difference in alpha hydrogen chemical shift ($\Delta\delta$)[18,20] in eq 1 below. The criteria set for the ^{1}H NMR screening measurement was $\Delta\delta > 0.02$,[18] and thus when a chiral solvent meets this requirement there might be some chiral recognition.

$$\Delta\delta = (\delta_{\text{reference}} - \delta_{\text{sample}}) \quad (1)$$

Table 1 contains the summarized experimental results of mandelic acid in the various screened solvents and their respective chemical shift in parts per million. Unfortunately, none of the nine chiral solvents fulfilled the criterion set. This reveals that the chiral solvent investigated had less interaction on the chiral system studied in terms of solution thermodynamics.

Raman Spectra. The Raman spectra of (*S*)- and (*R*)-mandelic acid in both (*S*)-ethyl lactate and (2*R*, 3*R*)-diethyl tartrate, respectively, are shown in Figures 3 and 4.

In both Figures 3 and 4, the Raman spectra of (*S*)- and (*R*)-mandelic acid in both (*S*)-ethyl lactate and (2*R*, 3*R*)-diethyl tartrate are identical to each other. Since there are no differences in the spectra of (*S*)- and (*R*)-mandelic acid in both chiral solvents, the results indicate again the absence of measurable interactions of the chiral molecules and the chiral solvent in the liquid phase. Since the results obtained from screening the various chiral solvents were similar, selection of the chiral solvents for further work was solely based on the availability and the price.

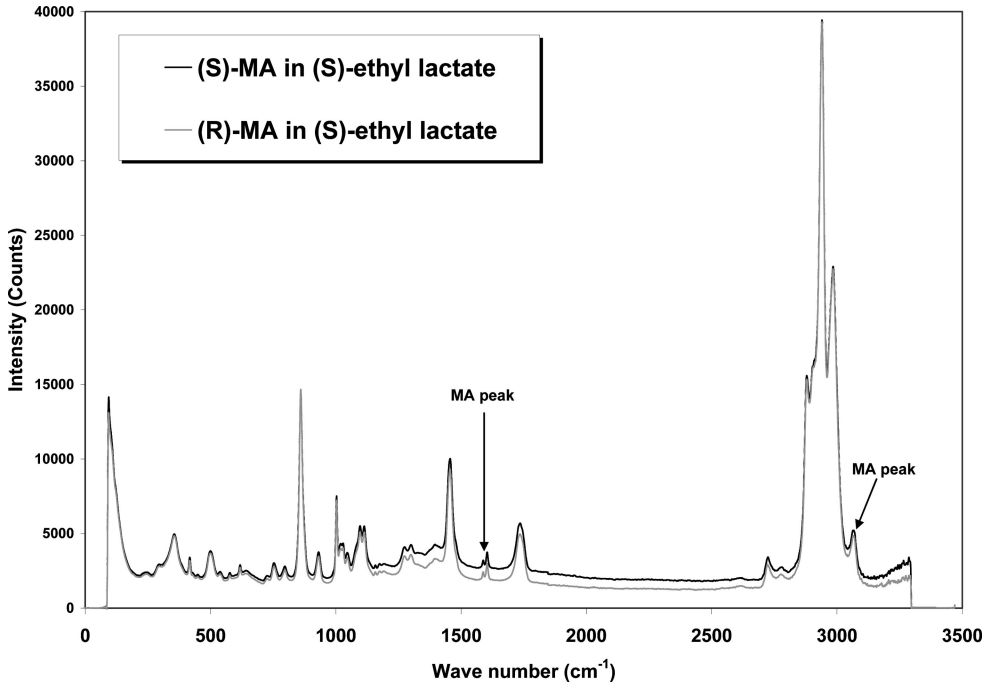

Figure 3. Raman spectra of (*S*)- and (*R*)-mandelic acid in (*S*)-ethyl lactate (liquid phase samples, and concentration of 8 wt %).

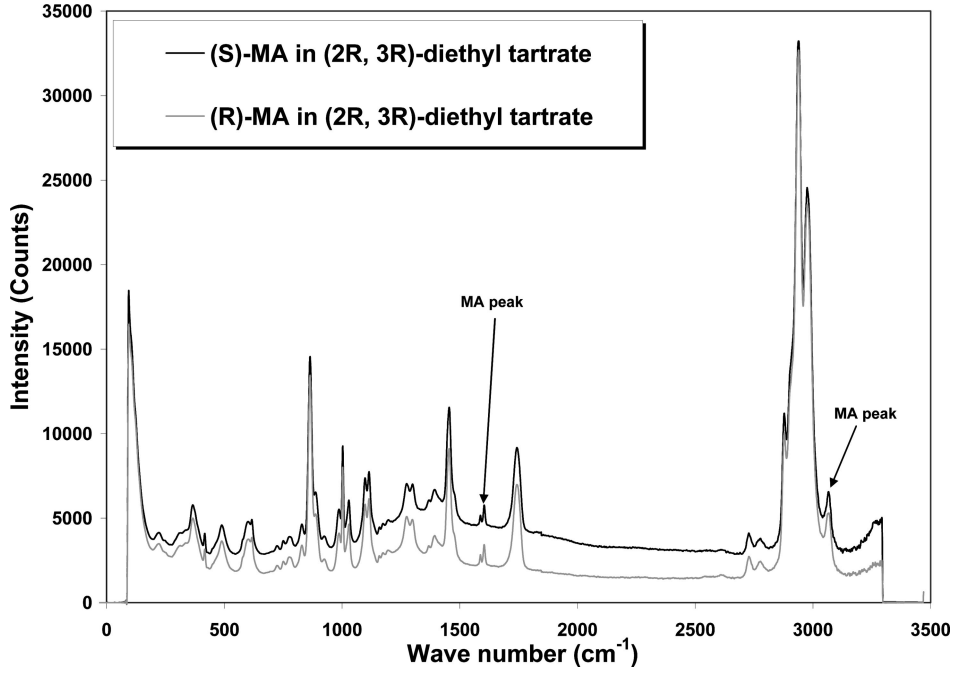

Figure 4. Raman spectra of (*S*)- and (*R*)-mandelic acid in (2*R*, 3*R*)-diethyl tartrate (liquid phase samples, and concentration of 8 wt %).

Ternary Phase Diagrams. Figures 5 and 6 illustrate the upper sections of the ternary phase diagrams of (*S*)-ethyl lactate and the two enantiomers of mandelic acid, and *N*-methylephedrine, respectively. Both figures show the typical behavior of compound and conglomerate forming system, respectively. In both cases, solubility isotherms are given at 5 and 15 °C. Further, Figures 7 and 8 show the upper sections of the ternary phase diagrams of both mandelic acid and *N*-methylephedrine in (2*R*, 3*R*)-diethyl tartrate, respectively. The ternary phase diagrams show solubility isotherms at 25 and 35 °C. These elevated temperatures were used in the case of (2*R*, 3*R*)-diethyl tartrate because its viscosity was high and the solutions were difficult to stir. In all ternary systems investigated, the solubilities of pure enantiomers, racemates, and the eutectic mixture increase with increasing temperature.

For both solvents ((*S*)-ethyl lactate and (2*R*, 3*R*)-diethyl tartrate), the solubilities of the mandelic acid enantiomers were found in the same range. For NME in (*S*)-ethyl lactate, a nonideal solubility behavior was observed; the solubility ratio of the racemic mixture to the single enantiomer is smaller than 2 (1.8 and 1.7 at 5 and 15 °C, respectively). The same is true in the case of NME in (2*R*, 3*R*)-diethyl tartrate, where the solubility ratio of the racemic mixture to the single enantiomer is smaller than 2 (1.7 and 1.6 at 25 and 35 °C, respectively). Furthermore, the solubility isotherms in both cases are not straight, but curved lines (Figures 6 and 8).

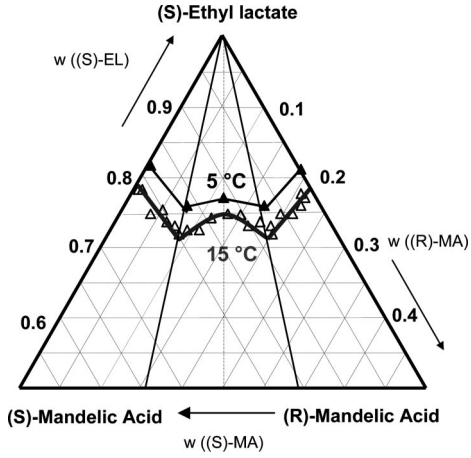

Figure 5. Ternary phase diagram for mandelic acid in (*S*)-ethyl lactate.

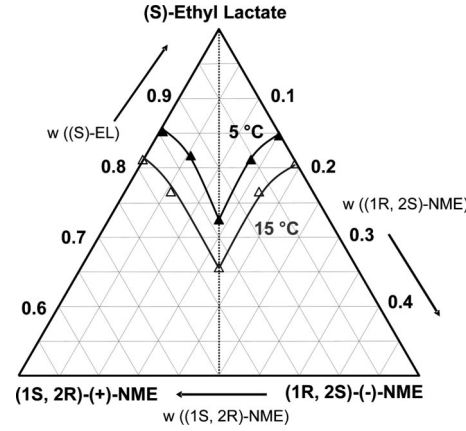

Figure 6. Ternary phase diagram for *N*-methylephedrine in (*S*)-ethyl lactate.

The phase diagrams for the two solvent systems ((*S*)-ethyl lactate and (2*R*, 3*R*)-diethyl tartrate) show no significant asymmetry for the temperatures studied. Even the eutectic composition of the mandelic acid enantiomers remains unchanged compared to water and the binary phase diagram (31/69 or 69/31).[22,8,23] Apparently, there exist no considerable specific interactions between the (*S*)-ethyl lactate, (2*R*, 3*R*)-diethyl tartrate and the chiral molecules inducing a recognizable symmetry shift in the phase diagrams. This is in agreement with the Raman results for mandelic acid discussed before.

From the results, it can therefore be deduced that there is no measurable chiral recognition in the liquid phase provided by the (*S*)-ethyl lactate and (2*R*, 3*R*)-diethyl tartrate.

Solid Phase Analysis. Figure 9depicts experimental XRPD patterns for solid phases obtained during the solubility measurements of mandelic acid in (S)-ethyl lactate at 15 °C. Different compositions of the chiral species are included. In each case the reflexes of the racemic compound and/or the mandelic acid enantiomer are clearly distinguishable. Typical reflexes characterizing the different species are indicated by gray to black colors, e.g., reflex at 6.0° is typical for the enantiomer, and reflex at 10.84° is typical for the racemic compound. The results for the eutectic compositions 38% ee show consistently reflexes of both the enantiomer and the racemate. No new phases are found.

Figure 10 illustrates experimental XRPD patterns for the solid phases obtained in solubility measurement for *N*-methylephedrine in (*S*)-ethyl lactate at 15 °C. Because *N*-methylephedrine in (*S*)-ethyl lactate is clearly a conglomerate forming system (Figure 6), the reflexes of the enantiomers and the racemic mixture must be identical. Deviations in the patterns would indicate the presence of different phases like a solvate or a polymorph. The various compositions really mimic the reference reflexes in the XRPD patterns, i.e., no new phases exist. Also the solid phases for both mandelic acid and *N*-methylephedrine in (2*R*, 3*R*)-diethyl tartrate were checked, and there were no additional or new phases formed in the crystal lattice.

Nucleation Experiments. In primary nucleation tests carried out for racemic-MA, (*S*)-MA, and (*R*)-MA in (*S*)-ethyl lactate, it was observed that there was a pronounced delay of the appearance of first crystals for (*R*)-MA, i.e., the induction time t_{ind} was very big compared with that of the (*S*)-MA and racemic-MA species, respectively. This nucleation delay behavior of the

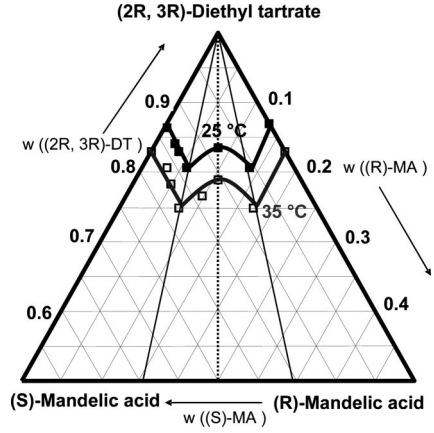

Figure 7. Ternary phase diagram for mandelic acid in (2*R*, 3*R*)-diethyl tartrate.

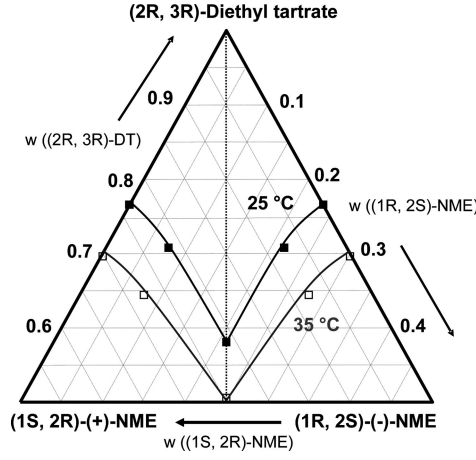

Figure 8. Ternary phase diagram for *N*-methylephedrine in (2*R*, 3*R*)-diethyl tartrate.

(*R*)-MA might be attributed to the stereospecific inhibition by the (*S*)-ethyl lactate and will be investigated in further work.

Conclusions

The ^{1}H NMR screening measurements and the Raman spectra show that the nine chiral solvents that were used for the study had no measurable influence on the chiral system studied. It

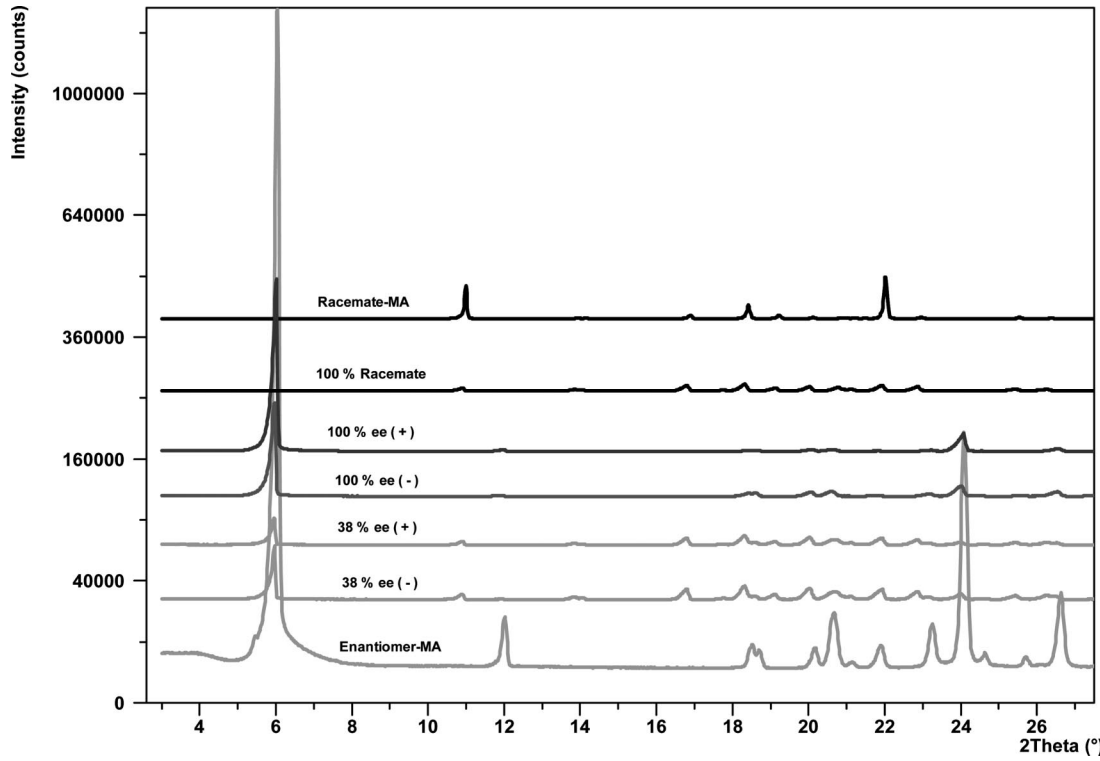

Figure 9. Experimental XRPD patterns for pure enantiomers and the racemate of mandelic acid, and the experimental compositions from (*S*)-ethyl lactate and mandelic acid at 15 °C.

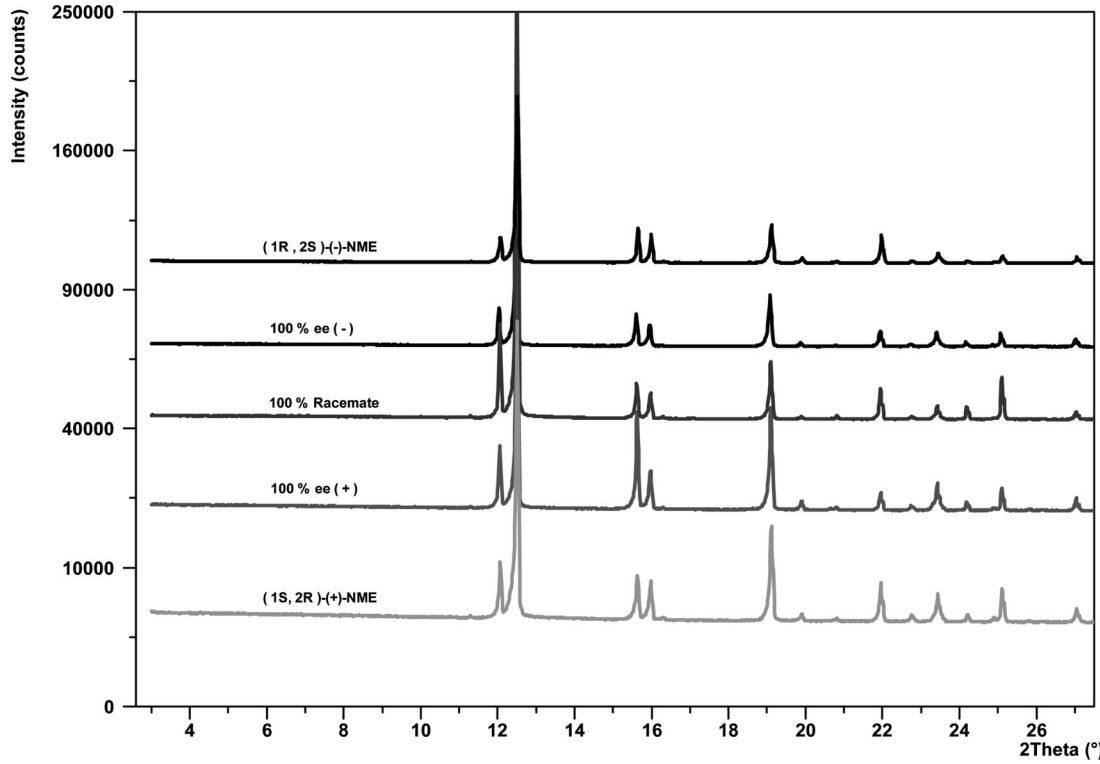

Figure 10. Experimental XRPD patterns for pure enantiomers and the racemate of *N*-methylephedrine, and the experimental compositions from (*S*)-ethyl lactate and *N*-methylephedrine at 15 °C.

was found that the investigated chiral solvents had less or no interaction to be exploited in thermodynamically based discrimination of the two enantiomers. The ternary solubility phase diagrams determined at different temperatures were indeed found to be symmetrical. This finally is a clear indication that the chiral solvents studied in this work had less or no influence on solution thermodynamics of the chiral systems mandelic acid and *N*-methylephedrine.

Future work will be directed toward chiral solvents that can provide stronger stereospecific interactions, because in principle

a classical three-point attachment should be favorable for chiral differentiation.[24] Molecular modeling of possible interactions between the chiral solvent and the chiral solutes should also support selecting suitable solvent candidates.

Additional work will be also focused on the application of nonclassical chiral solvents like chiral ionic liquids, because the viscous and more structured nature of ionic liquids might be more appropriate for chiral recognition.

During primary nucleation measurements, certain basic observations revealed that chiral solvent can have selective effects on kinetics. These kinetic effects and their potential to conduct enantioselective crystallization will be further explored. Part 2 of this work will discuss in more detail the kinetic effects observed in the nucleation experiments and how they can be successfully exploited for enantioselective crystallization.

Acknowledgment. The authors thank J. Kaufmann and L. Borchert at the Max Planck Institute in Magdeburg for the help in the experimental work. The authors thank BASF AG, Ludwigshafen, for support with samples of chiral solvents and Fonds der Chemischen Industrie for financial support.

Notations

Symbols

t_{ind}= induction time, time for first crystal to appear

$\delta_{reference}$ = chemical shift for the reference, ppm

δ_{sample} = chemical shift for the sample, ppm

$\Delta\delta$ = chemical shift difference, ppm

w = solubility, wt %

References

(1) Collins, A. N., Sheldrake, G. N., Crosby J., Eds.; *Chirality in Industry: The Commercial Manufacture and Applications of Optically Active Compounds*; Wiley & Sons: Chichester, U.K., 1992.
(2) Collins, A. N., Sheldrake, G. N., Crosby J., Eds.; *Chirality in Industry II: Developments in the Manufacture and Applications of Optical Active Compounds*; John Wiley & Sons: Chichester, U.K., 1997.
(3) Rouhi, A. M. *Chem. Eng. News* **2003**, *81*, 56–61.
(4) Reichardt, C. *Solvents and Solvent Effects in Organic Chemistry*, 3rd ed., Wiley VCH: Weinheim, Germany, 2003.
(5) Coquerel, G. In *Novel Optical Resolution Technologies*, 1st ed.; Sakai, N., Hirayama, R., Tamura, R., Eds.; Springer-Verlag: Berlin, 2007; Vol. 269, pp 1−51.
(6) Collet, A. *Enantiomer* **1999**, *4*, 157–172.
(7) Seebach, A.; Grandeury, A.; Seidel-Morgenstern, A. *Chem. Ing. Tech.* **2005**, *77*, 1005–1006.
(8) Lorenz, H.; Polenske, D.; Seidel-Morgenstern, A. *Chirality* **2006**, *18*, 828–840.
(9) Polenske, D.; Lorenz, H.; Seidel-Morgenstern, A. *Cryst. Growth Des.* **2007**, *7*, 1628–1634.
(10) Grandeury, A.; Petit, S.; Gouhier, G.; Agasse, V.; Coquerel, G. *Tetrahedron: Asymmetry* **2003**, *14*, 2143–2152.
(11) Jaques, J.; Collet, A.; Wilen, S. H. *Enantiomers, Racemates and Resolutions*; Krieger Publishing Company: Malabar, FL, 1994.
(12) Bosnich, B.; Watts, D. W. *J. Am. Chem. Soc.* **1968**, *90*, 6228–6230.
(13) Jones, H. O. *Proc. Cambridge Philos. Soc.* **1907**, *14*, 27–29.
(14) Mizumachi, K. *J. Coord. Chem.* **1973**, *3*, 191–192.
(15) Schipper, P. E.; Harrowell, P. R. *J. Am. Chem. Soc.* **1983**, *105*, 723–730.
(16) Yamamoto, M.; Yamamoto, Y. *Inorg. Nucl. Chem. Lett.* **1975**, *11*, 833–836.
(17) Amaya, K. *Bull. Chem. Soc. Jpn.* **1961**, *34*, 1803–1806.
(18) Dale, J. A.; Mosher, H. S. *J. Am. Chem. Soc.* **1973**, *95*, 512–519.
(19) Rouessac, F.; Rouessac, A. *CHEMICAL ANALYSIS: Modern Instrumentation Methods and Techniques*, 4th ed.; John Wiley & Sons: Chichester, U.K., 2000.
(20) Kobayashi, Y.; Hayashi, N.; Tan, C. H.; Kishi, Y. *Org. Lett.* **2001**, *3*, 2245–2248.
(21) Kobayashi, Y.; Hayashi, N.; Kishi, Y. *Org. Lett.* **2002**, *4*, 411–414.
(22) Lorenz, H.; Seidel-Morgenstern, A. *Thermochim. Acta* **2004**, *415*, 55–61.
(23) Lorenz, H.; Sapoundjiev, D.; Seidel-Morgenstern, A. *J. Chem. Eng. Data* **2002**, *47*, 1280–1284.
(24) Pispisa, B.; Venanzi, M. *J. Chem. Soc., Faraday Trans.* **1994**, *90*, 435–443.

CG800356V